

Elastic-electron-scattering cross sections for N_2 from 0 to 1000 eV. Energy-dependent exchange potentials

Jon Siegel and J. L. Dehmer

Argonne National Laboratory, Argonne, Illinois 60439

Dan Dill

Department of Chemistry, Boston University, Boston, Massachusetts 02215

(Received 14 February 1979; revised manuscript received 24 July 1979)

Integrated and differential cross sections for vibrationally elastic e^-N_2 scattering from 0 to 1000 eV are calculated by means of the continuum multiple-scattering method (CMSM) with the Hara free-electron-gas and semiclassical exchange approximations. The present results represent a significant improvement over earlier CMSM calculations employing the Slater $X\alpha$ exchange approximation. The physical basis for this improvement is discussed. Resonance structures appear at 2.4, 13, and 26 eV in the π_g , δ_g , and σ_u channels, respectively; however, the latter two are very weak and only the σ_u resonance has been observed in elastic scattering. Agreement between the present calculation and experiment is good over the entire energy range, although at fixed (equilibrium) internuclear distance, the π_g resonance is too narrow and high. The agreement at the π_g resonance is significantly improved by taking into account the effects of nuclear motion in the adiabatic nuclei approximation.

INTRODUCTION

Initial calculations of elastic e^-N_2 scattering^{1,2} using the continuum multiple-scattering method^{3,4} (CMSM) were reasonably successful in reproducing experimental integrated cross sections¹ over the wide energy range from threshold to 1000 eV, and differential cross sections² (DCSS) to 30 eV (DCS calculations were not carried beyond 30 eV). Further, they provided a simple physical interpretation of the dominant spectral features in terms of molecular shape resonances and the λ -composition of the continuum molecular wave functions. These calculations also displayed inherent limitations which stemmed, as we show here, not from the CMSM itself, but from the model potential employed with it,⁵ which was based on the Slater $X\alpha$ exchange approximation.⁶

The simplicity of the Slater $X\alpha$ treatment of exchange for bound-state problems is due to two particular features⁶: the treatment of the self-interaction and the averaging of the energy dependence of exchange over all bound levels. These combine to reduce an N -electron self-consistent-field (SCF) calculation from an N -potential problem to a one-potential problem. The success of this approach for bound-state problems in atoms⁷ and molecules⁸ attests to the usefulness of the approximations involved. However, for electron scattering this treatment of exchange is problematic.^{1,5} In particular, the potential (a) is energy independent, and hence cannot reflect the decrease in exchange with increasing electron kinetic energy, and (b) cannot be based on an SCF target wave function because the (e^- + neutral) system required

in this approach in order to cancel the self-interaction term⁶ is frequently not bound. Here we investigate alternative exchange approximations which (a) retain explicit dependence on the electron's kinetic energy and (b) are generated from SCF neutral target wave functions. The most useful of these are the Hara⁹ and semiclassical¹⁰ exchange approximations, which we document and compare to the Slater $X\alpha$ exchange approximation in Sec. II.

In Sec. III we evaluate cross sections for e^-N_2 scattering using the Hara and semiclassical exchange approximations. The calculations are carried out in the static-exchange-polarization (SEP) framework¹¹ in which the full potential V is given by

$$V(\vec{r}) = V_S(\vec{r}) + V_E(\vec{r}) + V_P(\vec{r}), \quad (1)$$

where V_S represents the electrostatic, V_E the exchange, and V_P the polarization components of the potential. We are thus able to study the effects of each of these terms separately. Note that due to the introduction of a self-interaction term, the $X\alpha$ potential combines V_S and V_E so that exchange effects cannot be isolated for study, e.g., at high energy where exchange becomes unimportant. Fixed-nuclei integrated cross sections from threshold to 1000 eV are presented and compared to experiment in this section, as are vibrationally averaged $v=0 \rightarrow 0$ cross sections through 1 Ry. The vibrational averaging is especially effective in reducing the excessive height of the π_g shape resonance to about the experimentally observed value (see Ref. 12 for a more detailed account of the effects of nuclear motion). Also pre-

sented are differential cross sections in both low (1.4–30 eV) and high (300, 400, and 500 eV) energy regions.

N_2 is frequently used as a prototype molecule in electron-scattering calculations, and this reinvestigation was conducted in that spirit. Based on the results presented here, CMSM calculations have been extended to a variety of molecules. Electron scattering by CO_2 , OCS , and CS_2 (Ref. 13) has been calculated using both the Hara and semiclassical exchange approximations. Results for these molecules support the results presented here for N_2 , which indicate that the Hara form provides more consistent agreement with experiment than does the semiclassical form. In addition, electron scattering calculations have been performed on H_2 ,¹⁴ SF_6 ,¹⁵ C_2H_4 ,¹⁶ and LiF (Ref. 16) (including the long-range dipole moment).

II. THEORY

In the single-particle model, the N -electron Schrödinger equation for a single-determinantal wave function is reduced, using projection or variational techniques,⁶ to N one-electron equations

$$[-\nabla^2 + V_s^i(\vec{r}) - \epsilon_i]u_i(\vec{r}) = \sum_{j \neq i} \delta(m_{s_i} m_{s_j}) u_j(\vec{r}) \int d\vec{r}' \frac{2u_j^*(\vec{r}')u_i(\vec{r}')}{|\vec{r} - \vec{r}'|} \quad (2)$$

for bound orbitals u_i , $i = 1$ to N , or, alternatively, to the single equation¹⁷

$$[-\nabla^2 + V_s(\vec{r}) - k_\infty^2]u_0(\vec{r}) = \sum_j \delta(m_{s_0} m_{s_j}) u_j(\vec{r}) \int d\vec{r}' \frac{2u_j^*(\vec{r}')u_0(\vec{r}')}{|\vec{r} - \vec{r}'|} \quad (3)$$

for continuum orbital u_0 . Here, V_s^i and V_s are the electrostatic potentials

$$V_s^i(\vec{r}) \equiv \sum_{j=1}^N \int d\vec{r}' \frac{2|u_j(\vec{r}')|^2}{|\vec{r} - \vec{r}'|} - \sum_k \frac{2Z_k}{|\vec{r} - \vec{R}_k|}, \quad (4)$$

$$V_s(\vec{r}) \equiv \sum_{j=1}^N \int d\vec{r}' \frac{2|u_j(\vec{r}')|^2}{|\vec{r} - \vec{r}'|} - \sum_k \frac{2Z_k}{|\vec{r} - \vec{R}_k|}. \quad (5)$$

Rydberg atomic units are used throughout. The index k represents the nuclei so that Z_k is the atomic number of the nucleus at position \vec{R}_k . ϵ_i is the eigenvalue of bound orbital u_i , and k_∞^2 is the kinetic energy of the continuum electron in orbital u_0 at infinity. m_{s_i} is the spin quantum number for orbital u_i . In both Eqs. (2) and (3) the terms on the right-hand side are *exchange terms* arising from the specification of the original wave function as a single Slater determinant.

We focus first on bound-state equation (2). The restriction $i \neq j$ in V_s^i , Eq. (4), reflects the physical

fact that an electron does not act on itself. However, Slater⁶ showed that by admitting the term with $i = j$, called the self-interaction, in *both* the left- and right-hand sums in Eq. (2), i.e.,

$$[-\nabla^2 + V_s(\vec{r}) - \epsilon_i]u_i(\vec{r}) = \sum_j \delta(m_{s_i} m_{s_j}) u_j(\vec{r}) \int d\vec{r}' \frac{2u_j^*(\vec{r}')u_i(\vec{r}')}{|\vec{r} - \vec{r}'|}, \quad (6)$$

considerable simplification is gained without disturbing the equality. All N orbitals u_i may now be calculated from the single electrostatic potential V_s rather than the N potentials V_s^i required by Eq. (2). Furthermore, the similar structure of Eqs. (3) and (6) means that the continuum and bound-state exchange approximations may be derived in parallel.

The first step in the determination of an exchange potential is the rearrangement of the right-hand side of Eqs. (3) and (6) to form

$$V_E^i(\vec{r})u_i(\vec{r}) = \left(\sum_j \delta(m_{s_i} m_{s_j}) \frac{u_j^*(\vec{r})u_i(\vec{r})}{|u_i(\vec{r})|^2} \right) \times \int d\vec{r}' \frac{2u_j^*(\vec{r}')u_i(\vec{r}')}{|\vec{r} - \vec{r}'|} u_i(\vec{r}). \quad (7)$$

Because u_i , the orbital sought, appears within the large parentheses, this equation does not yield an explicit expression for the exchange potential V_E^i . Continuum free-electron-gas (FEG) exchange approximations arise from evaluation of the expression in large parentheses using FEG orbitals, but the Slater bound-state approximation requires an additional step: The indexing of the bound-state exchange term V_E^i by i reflects the variation of the exchange interaction with the energy and form of the orbitals u_i . For an N -electron bound-state SCF problem this means that N potentials V , Eq. (1), differing only in their exchange component V_E^i , must be calculated at every iteration. To reduce this to a single potential, Slater *approximated* the N exchange potentials by an *averaged* potential⁶ $\langle V_E \rangle$ (one for closed shells; two for open shells representing, respectively, spin up \uparrow and down \downarrow). This is constructed as the weighted average

$$\langle V_{E\uparrow}(\vec{r}) \rangle \equiv \sum_{i\uparrow} V_E^i(\vec{r}) \left(|u_i(\vec{r})|^2 / \sum_{j\uparrow} |u_j(\vec{r})|^2 \right), \quad (8)$$

where the weight in large parentheses is the probability that an electron of spin up at position \vec{r} is in orbital i . (For closed shells, $\langle V_{E\uparrow} \rangle$ and $\langle V_{E\downarrow} \rangle$ will be equal.) As detailed below, the evaluation of Eq. (8) using FEG orbitals yields the original Slater exchange potential; multiplication by an empirical scaling coefficient α yields the so-called

$X\alpha$ potential.

The use of the Slater $X\alpha$ exchange approximation in electron-scattering calculations, in our original work^{1,2} on N₂ and by others,¹⁸⁻²⁰ assumes that $\langle V_E \rangle$ may be substituted for V_E^0 . As indicated earlier, this is problematic for two reasons: First, $\langle V_E \rangle$ subtracts an averaged self-interaction from the static potential V_S ; and second, the energy dependence accurately represented in Eq. (7) is needlessly replaced by the bound-state average. These two factors, the basis for the difficulties experienced in, e.g., Ref. 1, are actually *independent* of the free-electron-gas approximation and can be circumvented by evaluating V_E^0 directly using free-electron-gas orbitals.⁹

A. Free-electron-gas approximation

Evaluation of V_E^i using FEG orbitals yields ($i = 0$, continuum⁹; $i = 1$ to N , bound²¹)

$$V_E^{i,\text{FEG}}(\vec{r}) = -(4/\pi)k_F(\vec{r})f[\eta_i(\vec{r})], \quad (9)$$

$$\eta_i(\vec{r}) = k_i(\vec{r})/k_F(\vec{r}), \quad (10)$$

$$f(\eta) = \frac{1}{2} + [(1 - \eta^2)/(4\eta)] \ln |(1 + \eta)/(1 - \eta)|, \quad (11)$$

$$k_F(\vec{r}) = [3\pi^2\rho(\vec{r})]^{1/3}, \quad (12)$$

$$\rho(\vec{r}) = \sum_i |u_i(\vec{r})|^2, \quad (13)$$

where the sum in Eq. (13) extends over all occupied bound orbitals u_i ; k_F^2 is the Fermi energy in the FEG and corresponds to the local kinetic energy of the highest occupied level in the molecular case; and k_i^2 is a local orbital kinetic energy which is treated differently for the bound and continuum cases.

For bound levels, the FEG exchange interaction is averaged over k_i ($0 \leq k_i \leq k_F$) to yield the Slater exchange potential^{6,21}

$$\langle V_E^{\text{FEG}}(\vec{r}) \rangle = -6[(3/8\pi)\rho(\vec{r})]^{1/3}. \quad (14)$$

Multiplication of $\langle V_E^{\text{FEG}} \rangle$ times α yields the Slater $X\alpha$ exchange potential⁶

$$V_{X\alpha}(\vec{r}) = \alpha \langle V_E^{\text{FEG}}(\vec{r}) \rangle. \quad (15)$$

As Slater points out,⁶ the alternative derivation of Gasper²² and Kohn and Sham²³ and the calculations to Kmetko²⁴ and Schwarz,²⁵ make clear that values of α closer to $\frac{2}{3}$ than to unity yield wave functions closest to Hartree-Fock; values tabulated by Schwarz are used for the bound-state calculations in this work.

For continuum orbitals, k_0^2 determines the energy dependence of the exchange potential through Eq. (10). Hara⁹ proposed that this quantity be the sum of the local kinetic energy k_F^2 of the uppermost bound electron, plus the energy difference $|\epsilon_{\text{max}}|$ separating it from the conventional zero,

plus the energy k_∞^2 of the continuum electron above this zero:

$$k_{0,H}^2(\vec{r}) = k_F^2(\vec{r}) + |\epsilon_{\text{max}}| + k_\infty^2. \quad (16)$$

Here ϵ_{max} is given by the Hartree-Fock one-electron eigenvalue (the Koopmans-theorem ionization potential) of the uppermost bound electron. However, we approximate ϵ_{max} by the corresponding $X\alpha$ eigenvalue, which deviates slightly from the Hartree-Fock value due to the form of the $X\alpha$ total energy expression.⁶ Experience suggests that the final result is relatively insensitive to such minor changes in ϵ_{max} . Equation (16), together with Eqs. (9)–(13), define the Hara FEG exchange potential. A shortcoming of this exchange potential arises asymptotically where

$$\lim_{r \rightarrow \infty} k_{0,H}^2(\vec{r}) \sim |\epsilon_{\text{max}}| + k_\infty^2, \quad (17)$$

rather than the physical limit k_∞^2 . To correct this, Riley and Truhlar¹⁰ proposed the asymptotically adjusted FEG exchange based on the alternative definition

$$k_{0,AA}^2(\vec{r}) \equiv k_F^2(\vec{r}) + k_\infty^2. \quad (18)$$

This goes to the proper asymptotic limit, but simultaneously distorts the definition of the continuum electron's kinetic energy in the region of finite electron density, e.g., at threshold

$$\lim_{k_0^2 \rightarrow 0} k_{0,AA}^2(\vec{r}) \approx k_F^2(\vec{r}), \quad (19)$$

rather than the physical limit $k_F^2(\vec{r}) + |\epsilon_{\text{max}}|$, with the result that η is everywhere unity. Physically this means that a zero-energy electron and the uppermost bound electron are treated (for purposes of exchange) as if they have the same energy when, in fact, they differ in energy by $|\epsilon_{\text{max}}|$. Because this issue is most important for $k_F^2 \approx |\epsilon_{\text{max}}|$, where exchange plays a substantial role, whereas the asymptotic adjustment is concerned primarily with a region of space where exchange is negligible, it seems reasonable to us that the Hara form rather than the asymptotically adjusted form be adopted. For single-level systems (e.g., H₂ or He), however, where the replacement of the single term in the sum of Eq. (3) by an integral is an extreme approximation, the asymptotic adjustment plays a role in compensating for the underestimation of the exchange potential.⁵ This underestimation occurs because the FEG approximation assumes that the electrons are spread out in a range of energies at and below k_F^2 , whereas in reality they are all concentrated at k_F^2 . This stimulated the use of the "tuned FEG exchange" by Morrison and Collins¹¹ on electron-H₂ scattering. Because the asymptotic adjustment is not an exact compensation for this discrepancy, they found that empiri-

cal tuning of $|e_{\max}|$ between zero and the ionization potential was necessary for best results. Consistent with this reasoning, they also found that no adjustment at all was necessary for the multilevel systems N_2 (Ref. 11) and CO_2 (Ref. 26).

B. Semiclassical exchange

The derivation of the semiclassical exchange potential is given by Riely and Truhlar in Ref. 10; we briefly review it here (for closed shells) by way of contrast with the FEG approximations. We wish to approximate the exchange term on the right-hand side of Eq. (3) as a potential, i.e.,

$$V_E^0(\vec{r})u_0(\vec{r}) \approx \sum_j \delta(m_{s_0}m_{s_j})u_j(\vec{r}) \times \int d\vec{r}' \frac{2u_i^*(\vec{r}')u_0(\vec{r}')}{|\vec{r}-\vec{r}'|} \quad (20)$$

To do this, the integral in Eq. (20) is represented as the product

$$A_i(\vec{r})u_0(\vec{r}) \equiv \int d\vec{r}' \frac{2u_i^*(\vec{r}')u_0(\vec{r}')}{|\vec{r}-\vec{r}'|} \quad (21)$$

of an assumed slowly varying exchange amplitude A_i and the continuum orbital u_0 . The expression of A_i in terms of known quantities yields the semiclassical exchange potential. To accomplish this, one operates on both sides of Eq. (21) with ∇^2 ; on the left-hand side one uses the product rule and on the right-hand side, recognizing the electrostatic potential due to the exchange charge density $u_i^*u_0$, one employs Poisson's equation. The result is

$$[\nabla^2 A_i(\vec{r})]u_0(\vec{r}) + 2[\vec{\nabla} A_i(\vec{r})] \cdot [\vec{\nabla} u_0(\vec{r})] + A_i(\vec{r})\nabla^2 u_0(\vec{r}) = -4\pi[2u_i^*(\vec{r})u_0(\vec{r})]. \quad (22)$$

The continuum Schrödinger equation furnishes an expression for $\nabla^2 u_0$ if one writes

$$[-\nabla^2 - k_{0,SCE}^2(\vec{r})]u_0(\vec{r}) = 0, \quad (23)$$

$$k_{0,SCE}^2(\vec{r}) = k_\infty^2 - V_S(\vec{r}) - V_E(\vec{r}), \quad (24)$$

where V_E is the desired exchange potential. By substituting $-k_{0,SCE}^2 u_0$ for $\nabla^2 u_0$ in Eq. (21), Riley and Truhlar expand the amplitude A_i in inverse powers of $k_{0,SCE}^2$ as

$$A_i(\vec{r}) = 8\pi u_i^*(\vec{r})/k_{0,SCE}^2(\vec{r}) + 2[\vec{\nabla} u_0(\vec{r})/u_0(\vec{r})] \cdot [8\pi \vec{\nabla} u_i^*(\vec{r})]/k_{0,SCE}^4 + \dots \quad (25)$$

This expansion is truncated at the first term, which will be valid either if $k_{0,SCE}^2 \gg 1$ or if A is a slowly varying function of \vec{r} . Finally, the expression for A_i is substituted into Eq. (21) and then into Eq. (20). Substitution of the definition (24) of

$k_{0,SCE}^2$ into this relation yields a quadratic equation for V_E with two roots. The root for which $V_E^0 = 0$ for $k_\infty^2 = \infty$ is

$$V_E^{0,SCE}(\vec{r}) = \frac{1}{2}[k_\infty^2 - V_S(\vec{r})] - \frac{1}{2}\{[k_\infty^2 - V_S(\vec{r})]^2 + \beta(\vec{r})\}^{1/2}, \quad (26)$$

$$\beta(\vec{r}) = 16\pi\rho(\vec{r}), \quad (27)$$

where ρ is defined by Eq. (13).

III. RESULTS

We employ self-consistent MS- $X\alpha$ wave functions for the ground state of N_2 to generate V_S , Eq. (5), and ρ , Eq. (13). These are generated from the bound-state code provided to us by Keith Johnson.⁸ The N-N internuclear distance of $2.0744a_0$ (Ref. 27) fixes the sphere radii at $2.0744a_0$ (outer sphere) and $1.0372a_0$ (nitrogen spheres). The Schwarz value²⁵ $\alpha = 0.75197$ was used in all regions, and the Latter tail²⁸ was applied beyond the outer sphere during the SCF process. Partial waves up to $l=4$ on all sites for σ_g , and $l=5$ for σ_u and π_u , were included except for the $1\sigma_g$ and $1\sigma_u$ which were treated as free core levels.⁸ This represents a high degree of convergence in l : The highest l component of each state contained less than 0.2% of the charge for that state except for the valence $3\sigma_g$ for which the highest l component contained 1.3%. The convergence criterion for self-consistency of the potential was 1.0×10^{-3} . Two quantities function as indicators of the ability of the multiple-scattering model to approximate Hartree-Fock solutions. The first is the total energy⁶ $\langle EX\alpha \rangle$, which may be compared directly to the Hartree-Fock (HF) total energy. The present $X\alpha$ calculation yielded a total energy of -215.73 Ry compared to Nesbet's HF energy²⁹ of -217.94826 Ry, giving the ratio $\langle EX\alpha \rangle / \langle EHF \rangle = 0.9898$. The second indicator is the virial ratio $-\langle EX\alpha \rangle / T$ of total and kinetic energies.^{6,8} This ratio equals 1 if the Coulomb forces are represented exactly. To the extent that the constant potential in the interstitial region or the truncation of the potential expansion in partial waves distorts this representation, the virial ratio will deviate from unity. The value obtained for the N_2 calculation is 0.9784. (The long-range quadrupole moment, also used to judge wave functions, was not evaluated in the monopole-approximation calculations of this study.)

Continuum calculations were performed using the CMSM in the monopole approximation, as described by Dill and Dehmer.^{1,3} Convergence of the partial-wave expansion of the continuum wave functions was determined from the eigenphase sum.¹ Partial waves ($l_{\text{outer sphere}}, l_N, \lambda$) required for conver-

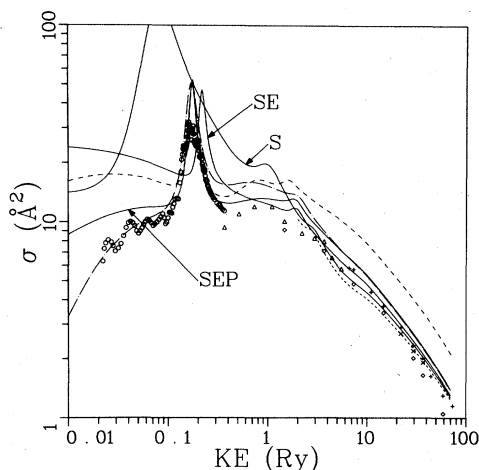


FIG. 1. Integrated cross sections for elastic e^- -N₂ scattering comparing various exchange approximations. Theoretical results include Hara exchange, —; semiclassical exchange, - · - ·; Slater $X\alpha$ potential A, ---; and B, ---- (the latter two are reproduced from Ref. 1). Unless labeled otherwise, calculations were performed in the SEP approximation. Comparison is made to the following experimental data: Golden (Ref. 30), ○; Bromberg (Ref. 31), ✕; Dubois and Rudd (Ref. 32), ◇; Srivastava *et al.* (Ref. 33), △; and Hermann *et al.* (Ref. 34), +.

gence to 0.006 rad are (12, 8, 7) to 2 Ry, (14, 10, 9) to 5 Ry, and (18, 12, 12) to 70 Ry. For the Hara exchange, ϵ_{\max} was taken as the highest $X\alpha$ eigenvalue -0.75898 of the $3\sigma_g$ orbital. Calculations using the largest of these bases took 8 sec/energy on an IBM 370/195.

Figure 1 contrasts the results of the three exchange potentials—Hara (—), semiclassical (- · - ·), and Slater $X\alpha$ potentials A (---) and B (----) of Ref. 1—over the energy range from 0.01 to 70 Ry (approximately 1 keV). The Hara exchange results are shown in the S, SE, and SEP approximations; we will discuss the SEP results here in comparison with semiclassical and

Slater $X\alpha$ exchange, and discuss the effects of V_E and V_P later on in this section. Polarization is included in region III only. We use the form

$$V_P = (-\alpha_0/r^4)\{1 - \exp[-(r/r_0)^6]\},$$

where $\alpha_0 = 12a_0^3$ is the monopole polarizability³⁵ and r_0 is a cutoff parameter which is determined empirically. For both SEP continuum exchange calculations shown in Fig. 1, the polarization cutoff parameter r_0 has been adjusted to position the π_g resonance at the experimentally observed energy of 2.39 eV.³⁰ For Hara exchange this required $r_0 = 2.90a_0$; for semiclassical exchange $r_0 = 3.10a_0$. For comparison, the Hara exchange calculation of Morrison and Collins¹¹ used $2.341a_0$, and a study by Buckley and Burke³⁶ required $2.308a_0$. Buckley and Burke used an exact exchange algorithm but neglected exchange with the core $1\sigma_g$ and $1\sigma_u$ molecular orbitals. A recent study by Collins *et al.*³⁷ showed that, due to the substantial amplitude of the resonant state in the core region, inclusion of this exchange interaction pulls the resonance in from 4.35 to 3.77 eV. Thus the Buckley-Burke value of $2.308a_0$ must be regarded as a lower limit for r_0 using exact exchange. For Slater $X\alpha$ potential A, no cutoff function was used as explained in Ref. 1, and potential B was constructed without polarization. Note that our use of a single cutoff radius over the range from threshold to 1000 eV is a very severe test of this one-parameter polarization potential as it is optimized for only one channel at one energy. This is discussed further in connection with the net effect of V_P later in this section.

Both the Hara and semiclassical exchange approximations yield semiquantitative results throughout the entire energy range shown in Fig. 1, and constitute a clear improvement over the Slater $X\alpha$ two-potential treatment of Ref. 1. Semiclassical exchange suppresses the σ_g partial cross section at low kinetic energy [see Fig. 2(a)] and so is more accurate than Hara exchange below

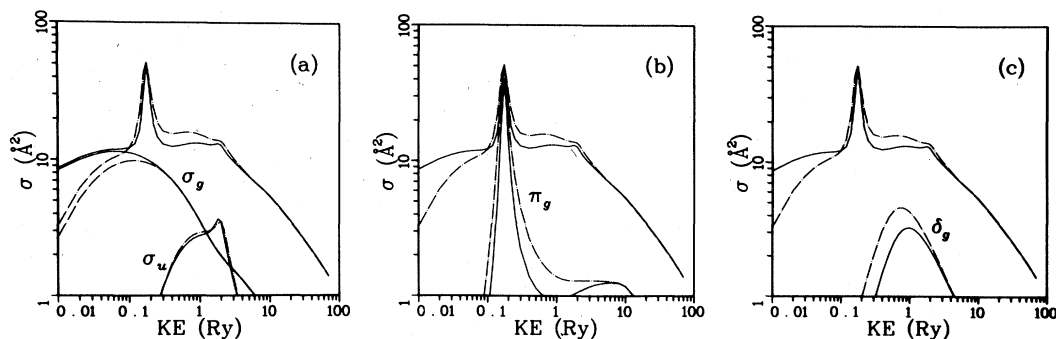


FIG. 2. Comparison of Hara (—) and semiclassical (- · - ·) exchange results in the SEP approximation. Each frame includes the total cross sections plus the indicated partial cross sections.

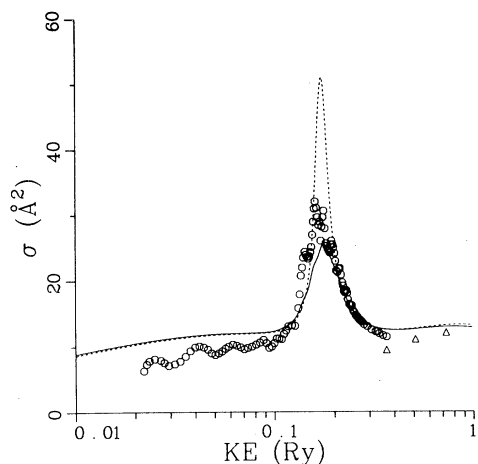


FIG. 3. Effects of nuclear motion on $e^- - N_2$ scattering near the π_g resonance. The adiabatically R -averaged cross section and the fixed-nuclei cross section are represented by solid and dashed lines, respectively. Experimental data are represented by symbols according to the convention in Fig. 1.

the π_g resonance. At the π_g resonance [Fig. 2(b)], the two approximations yield similar results. Just above the π_g resonance the semiclassical result exceeds experiment due to contributions from both the resonant δ_g [Fig. 2(c)] and post-resonant π_g components. Finally, above 8 to 10 Ry, the two exchange treatments yield identical results.

The cross section at the π_g resonance exceeds 50 \AA^2 for all three exchange approximations shown in Fig. 1. Similar results were obtained by Buckley and Burke³⁶ and Morrison and Collins.¹¹ This excess above the experimental value³⁰ of $\sim 30 \text{ \AA}^2$ is due to the fixed-nuclei approximation, and averaging over nuclear motion brings the results into good agreement with experiment. Figure 3 shows our R -averaged results for the $v = 0 \rightarrow 0$ transition in the vicinity of the π_g resonance (solid line). Details of the calculation of vibrationally averaged and vibrationally inelastic processes will be given separately.¹² Note that the vibrational fine structure on the π_g resonance arises from nonadiabatic coupling of electronic and nuclear motion³⁸ not accounted for by our averaging procedure.

The σ_u shape resonance [Fig. 2(a)] originally predicted by us in Ref. 1 has recently been observed by Kennerly³⁹ as a broad peak centered at 21 eV in the elastic scattering spectrum, displaced slightly from the current calculation's center at 26 eV. CMSM calculations, to be reported in detail separately,¹² predict this resonance to be active in vibrational excitation as well, as seen in the experimental results of Pavlovic *et al.*⁴⁰ The δ_g resonance at 13 eV, however, is apparently

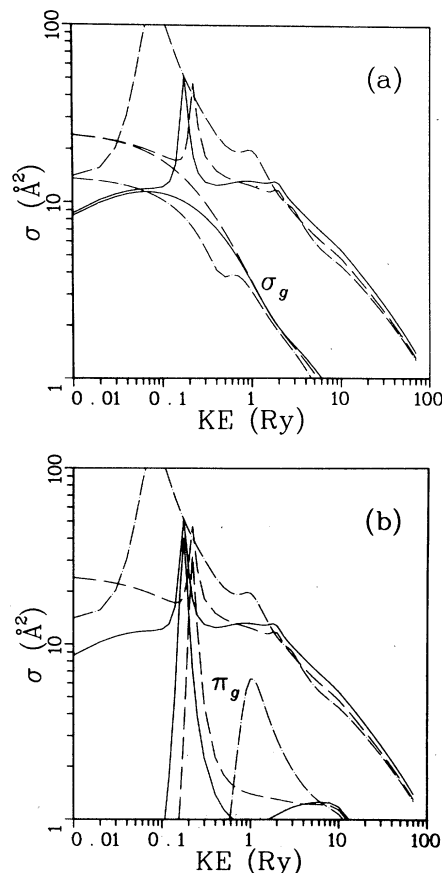


FIG. 4. Hara exchange results in the SEP (—), SE(---), and S(-·-·) approximations. Total cross sections for all three approximations are shown in each frame, together with the indicated partial cross sections.

too weak to observe in elastic scattering.³⁹ This is more consistent with the Hara results in Fig. 2(c) in which the δ_g resonance is significantly weaker and barely detectable in the total cross section. Moreover, the δ_g resonance is not active in vibrational excitation owing to its weakness and orientation away from the molecular axis.

Because Slater $X\alpha$ potential B (short dashes in Fig. 1) corresponds to finite exchange at high energy, when in fact exchange should vanish there, its good agreement with experiment is fortuitous. We will demonstrate shortly that *no* exchange is necessary in this energy region in order to obtain such good agreement. That potential B does so well using $\alpha = \frac{2}{3}$ indicates that its repulsive negative-ion character substantially cancels this exchange component. Differential cross section calculations¹⁶ using potential B at 25 and 30 eV verify that its representation is not as good as suggested by Fig. 1.

Figures 1 and 4 illustrate the effects of the V_p

and V_p terms in the SEP potential. The solid lines of Fig. 1 show the Hara exchange total cross sections in the SEP, SE, and S approximations and compare them to experiment, and Fig. 4 isolates the σ_g and π_g components. Comparing the SEP and SE results (solid and dashed lines, respectively) in Fig. 4, we see that the polarization interaction has three effects: First, it significantly reduces the σ_g cross section at low energy [Fig. 4(a)], bringing it into better agreement with experiment. Second, it shifts the π_g resonance [Fig. 4(b)] by 0.6 eV from 3.0 eV to the experimental energy of 2.39 eV without significantly changing its shape. Third, the adiabatic form of the polarization potential used here overestimates the response of the target to a fast electron, i.e., above 8 to 10 Ry the SE results agree better with experiment (Fig. 1). However, high-energy DCS results discussed below show V_p is required to

reproduce the large forward-scattering component, although it has negligible effect at intermediate and large angles. Clearly, optimization of the single-parameter polarization potential for one channel and one energy is not sufficient to obtain the best results for all scattering channels and over the broad energy range treated here; nor would it be useful to perform multiple optimizations in a study with the present broad scope. Nevertheless, we have shown that selecting a single, reasonable value of r_0 is sufficient, in the context of the CMSM, to produce realistic cross sections for the entire scattering process over four decades of the energy spectrum. Eventually the ambiguities surrounding treatment of V_p must be removed via the development of an energy- and symmetry-dependent polarization potential.

The electrostatic potential alone (dash-dotted line in Fig. 4) is not attractive enough to bind the

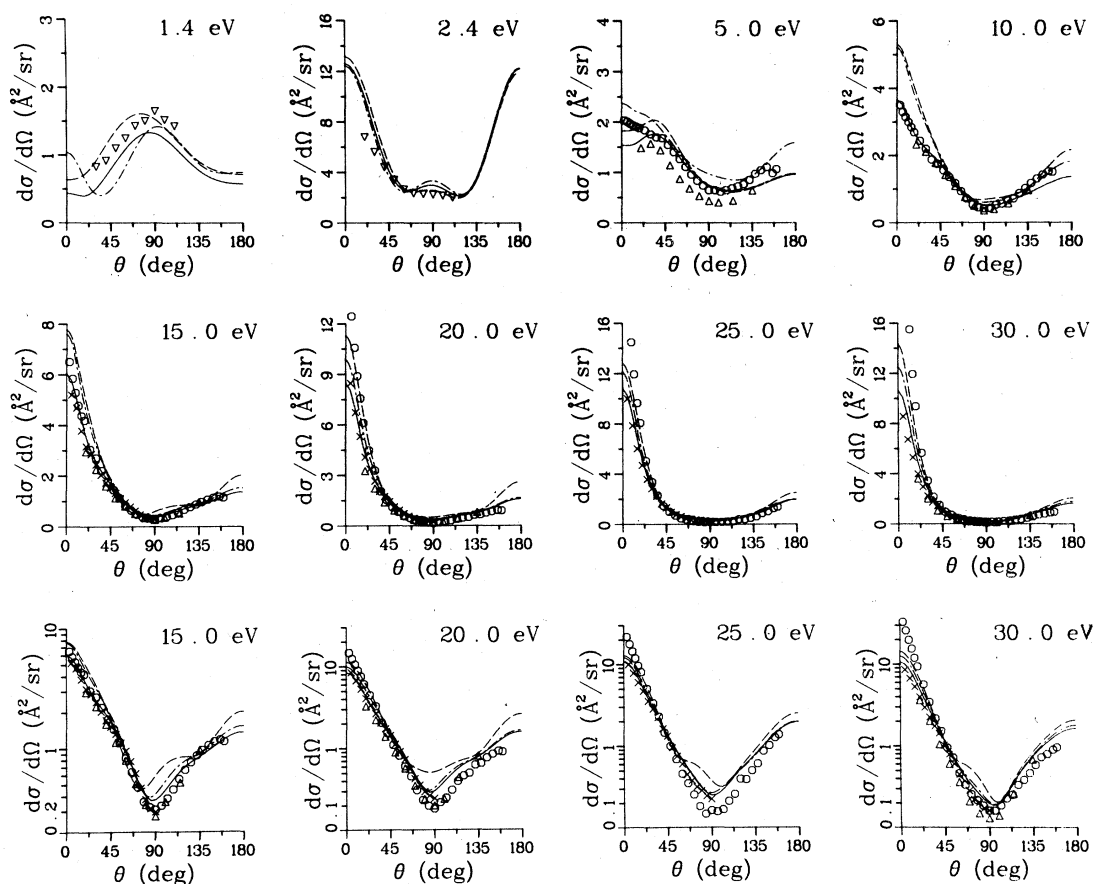


FIG. 5. Differential cross sections for elastic e^-N_2 scattering at selected energies below 30 eV. Note that the middle and bottom rows display identical data on linear and logarithmic abscissae, respectively. Theoretical curves include Hara exchange (—), semiclassical exchange (— · —), and Slater $X\alpha$ potential A of Ref. 1 (---). Relative experimental results are normalized to the Hara exchange calculation at the energy and angle noted: Ehrhardt and Willmann (Ref. 41), ∇ , normalized at 2.4 eV, 50° ; Shyn *et al.* (Ref. 42), \circ , normalized at 5 eV, 30° ; Srivastava *et al.* (Ref. 33), Δ , in absolute units as given by the authors; and Finn and Doering (Ref. 43), \times , normalized at 15 eV, 30° .

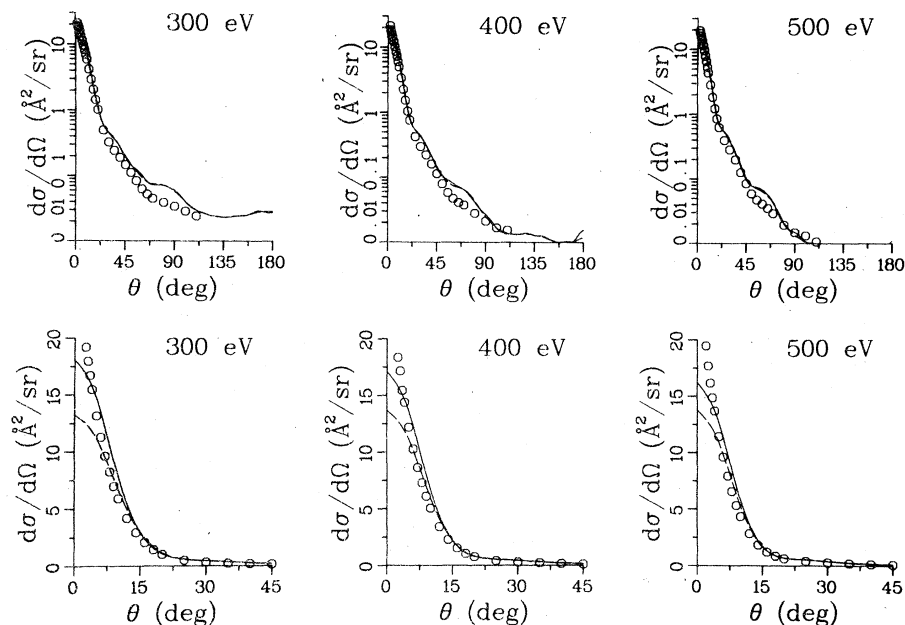


FIG. 6. Differential cross sections for elastic e^- - N_2 scattering at 300, 400, and 500 eV. Theoretical curves represent SEP (—) and SE (---) calculations using the Hara exchange approximation. Symbols denote the absolute experimental data of Bromberg (Ref. 31).

π_u bonding molecular orbital, which appears here as a large π_u resonance centered at 0.08 Ry. The σ_g component [Fig. 4(a)] has a shoulder at 0.6 Ry, which is possibly the origin of the enhanced σ_g threshold cross section in the SEP and SE results. Finally, the π_g resonance [Fig. 4(b)] is moved up by more than 0.76 Ry compared to the SEP position, occurring at 1.0 Ry, and its magnitude is reduced from ~ 40 to ~ 7 Å². The effect of exchange is small above ~ 10 Ry, as shown by the proximity of the (dashed) static-exchange and (dash-dotted) static total cross sections. This confirms that the current model goes to the proper limit of vanishing exchange at high energy.

Having studied the effects of variations of V_E and V_P in the context of the CMSM, we wish to stress a most important conclusion. That is, using either the Hara or semiclassical forms of V_E and either including or omitting V_P , we observe an identical pattern of low- and intermediate-energy shape resonances. Although these various choices shift the resonance positions somewhat and alter the resonance strengths, only the complete neglect of V_E led to a qualitatively incorrect result.

Figure 5 shows the differential cross sections at eight energies between 1.4 and 30.0 eV. The calculation of the DCS was performed as in Ref. 2, and Fig. 5 is identical in layout to Fig. 2 of Ref. 2, except that the results of other theories have been omitted for clarity, and the relative experimental results have been renormalized to the Hara exchange results at the energies and angles indicated in the caption. Hara exchange results are shown by

a solid line, semiclassical by a dash-dotted line, and potential A by long dashes; experimental points are represented by symbols. Figure 5 shows that both Hara and semiclassical exchange provide a realistic representation of the DCS throughout this energy range, with the Hara noticeably better mainly at 1.4, 5.0, and 10 eV. At 1.4 eV, the semiclassical result appears to overestimate forward scattering. At 5.0 eV only one set of data shows the turnover at small angles predicted by the Hara and potential A calculations; however, the small-angle ($\theta < 24^\circ$) results of Shyn et al.⁴¹ (circles) are extrapolated rather than measured, and are thus unable to show this feature. Semiclassical exchange fails to reproduce the turnover and shows distortions at intermediate and large angles as well, possibly arising from the excessive δ_g component shown in Fig. 2(c). Below 10 eV, the Hara and, to some extent, the semiclassical exchange results show only slight improvement over potential A . It is in the 15–30 eV DCSs, where potential A was unable to reproduce the minimum at 90° , that the continuum exchange shows substantial improvement. Here both Hara and semiclassical exchange yield clean minima at 90° , easily visible in the log plots in Fig. 5.

The DCSs at 300, 400, and 500 eV are shown in Fig. 6, along with the absolute experimental data of Bromberg.³¹ These were calculated using the Hara exchange approximation only; based on the results shown in Fig. 5 it is unlikely that semiclassical exchange would show any difference. They were, however, done with (—) and without (---) polarization. In the upper row of Fig. 6, the

agreement with experiment is very close in slope and magnitude at all three energies; however, the calculated spectra show a bump around 90° which is not clearly seen in the experimental data. Even here the deviation is only 0.03–0.05 Å²/sr. Polarization has negligible effect except for small-angle scattering; however in the forward direction polarization significantly increases the cross section, as shown in the bottom row of Fig. 6. The calculations required up to $j_t = 8$ in the DCS expansion [Eq. (1) of Ref. 2] for convergence to better than 1% at 300 and 400 eV, and 1.5% at 500 eV. Extension to $j_t = 10$ at 300 eV resulted in changes barely noticeable in the final result. Because this more than doubled the computer time compared to $j_t = 8$ calculations, this extension was not tried at 400 and 500 eV.

IV. CONCLUSIONS

The central message of this work is that continuum exchange approximations (and in particular the Hara exchange approximation), rather than the Slater $X\alpha$ exchange approximation, are necessary to construct potentials which yield realistic representations of electron-molecule scattering over large energy ranges. While our results pertain specifically to the CMSM, other workers^{9–11,26} have shown the importance of continuum exchange approximations in the context of other molecular

models. Our experience here, in Ref. 1 with N₂, and in exploratory calculations on CO₂, OCS, CS₂, and SF₆, indicates that excessive tuning of potentials based on the Slater $X\alpha$ exchange approximation is required to reproduce experiment; and even then for some molecules agreement is not satisfactory. Using the Hara exchange approximation, on the other hand, we have obtained qualitatively correct static-exchange results (see, e.g., Fig. 1) in each case, without any adjustment of the molecular potential (no parameter of the bound state calculation, e.g., α , was adjusted to improve the continuum calculation). Then, by including the polarization potential with the single adjustable parameter r_0 , these results become semiquantitative. Thus, we feel that continuum exchange approximations provide a reliable basis with which to conduct predictive studies of electron-molecule scattering using the continuum multiple-scattering method.

ACKNOWLEDGMENTS

This work was performed in part under the auspices of the U. S. DOE and NSF Grant No. CHE78-08707. Acknowledgment is also made to the donors of the Petroleum Research Fund, administered by the American Chemical Society, for the partial support of this research.

-
- ¹D. Dill and J. L. Dehmer, *Phys. Rev. A* **16**, 1423 (1977).
²J. Siegel, D. Dill, and J. L. Dehmer, *Phys. Rev. A* **17**, 2106 (1978).
³D. Dill and J. L. Dehmer, *J. Chem. Phys.* **61**, 692 (1974).
⁴J. Siegel, D. Dill, and J. L. Dehmer, *J. Chem. Phys.* **64**, 3204 (1976).
⁵J. Siegel, Ph.D. thesis (Boston University, 1979) (unpublished).
⁶J. C. Slater, *Quantum Theory of Molecules and Solids*, (McGraw-Hill, New York, 1974), Vol. IV.
⁷F. Herman and S. Skillman, *Atomic Structure Calculations* (Prentice-Hall, Englewood Cliffs, 1963).
⁸See, e.g., K. H. Johnson, in *Advances in Quantum Chemistry*, edited by P. O. Löwdin (Academic, New York, 1973), Vol. 7, p. 143.
⁹S. Hara, *J. Phys. Soc. Jpn.* **22**, 710 (1967).
¹⁰M. E. Riley and D. G. Truhlar, *J. Chem. Phys.* **63**, 2182 (1975).
¹¹M. A. Morrison and L. A. Collins, *Phys. Rev. A* **17**, 918 (1978).
¹²J. L. Dehmer, J. Siegel, J. Welch, and D. Dill, *Phys. Rev. A* **21**, 101 (1980).
¹³M. G. Lynch, D. Dill, J. Siegel, and J. L. Dehmer, *J. Chem. Phys.* (to be published).
¹⁴J. Welch, Undergraduate Distinction Work Report (Department of Chemistry, Boston University, 1978) (unpublished).
¹⁵J. L. Dehmer, J. Siegel, and D. Dill, *J. Chem. Phys.* **69**, 5205 (1978).
¹⁶J. Siegel, J. L. Dehmer, and D. Dill (unpublished).
¹⁷See, e.g., Ref. 11.
¹⁸See, e.g., Refs. 6–10 of Ref. 10.
¹⁹J. W. Davenport, Ph. D. thesis (University of Pennsylvania, 1976) (unpublished).
²⁰J. W. Davenport, W. Ho, and J. R. Schrieffer, *Phys. Rev. B* **17**, 3115 (1978).
²¹J. C. Slater, *Quantum Theory of Atomic Structure* (McGraw-Hill, New York, 1960), Vol. I, Appendix 22.
²²R. Gaspar, *Acta Phys. Acad. Sci. Hung.* **3**, 263 (1954), as cited in Ref. 6.
²³W. Kohn and L. J. Sham, *Phys. Rev.* **140**, A1133 (1965).
²⁴E. A. Kmetko, *Phys. Rev. A* **1**, 37 (1970).
²⁵K. Schwarz, *Phys. Rev. B* **5**, 2466 (1972).
²⁶M. A. Morrison, N. F. Lane, and L. A. Collins, *Phys. Rev. A* **15**, 2186 (1977).
²⁷B. Rosen, *Spectroscopic Data Relative to Diatomic Molecules* (Pergamon, Oxford, 1970).
²⁸R. Latter, *Phys. Rev.* **99**, 510 (1955).
²⁹R. K. Nesbet, *J. Chem. Phys.* **40**, 3619 (1964).
³⁰D. E. Golden, *Phys. Rev. Lett.* **17**, 847 (1966).
³¹J. P. Bromberg, *J. Chem. Phys.* **52**, 1243 (1970).
³²R. D. Dubois and M. E. Rudd, *J. Phys. B* **9**, 2657 (1976).
³³S. K. Srivastava, A. Chutjian, and S. Trajmar, *J. Chem. Phys.* **64**, 1340 (1976).

- ³⁴D. Hermann, K. Jost, and J. Kessler, *J. Chem. Phys.* 64, 1 (1976).
- ³⁵Landolt-Börnstein, *Zahlenwerte und Funktionen* (Springer, Berlin, 1951), Vol. I, Pt. 3, p. 509 *et seq.*
- ³⁶B. D. Buckley and P. G. Burke, *J. Phys. B* 10, 725 (1977).
- ³⁷L. A. Collins, W. D. Robb, and M. A. Morrison, *J. Phys. B* 11, L777 (1978).
- ³⁸See, e.g., N. Chandra and A. Temkin, *Phys. Rev. A* 13, 188 (1976); D. T. Birtwistle and A. Herzenberg, *J. Phys. B* 4, 53 (1971).
- ³⁹R. E. Kennerly, *Phys. Rev. A* (to be published).
- ⁴⁰Z. Pavlovic, M. J. W. Boness, A. Herzenberg, and G. J. Schulz, *Phys. Rev. A* 6, 676 (1972).
- ⁴¹W. Ehrhardt and K. Willmann, *Z. Phys.* 204, 462 (1967).
- ⁴²T. W. Shyn, R. S. Stolarski, and G. R. Carignan, *Phys. Rev. A* 6, 1002 (1972).
- ⁴³T. G. Finn and G. P. Doering, *J. Chem. Phys.* 63, 4399 (1975).